



## Tropical Atlantic Biases in CCSM4

SEMYON A. GRODSKY, JAMES A. CARTON, AND SUMANT NIGAM

*Department of Atmospheric and Oceanic Science, University of Maryland, College Park, College Park, Maryland*

YUKO M. OKUMURA

*National Center for Atmospheric Research,\* Boulder, Colorado*

(Manuscript received 8 June 2011, in final form 25 October 2011)

### ABSTRACT

This paper focuses on diagnosing biases in the seasonal climate of the tropical Atlantic in the twentieth-century simulation of the Community Climate System Model, version 4 (CCSM4). The biases appear in both atmospheric and oceanic components. Mean sea level pressure is erroneously high by a few millibars in the subtropical highs and erroneously low in the polar lows (similar to CCSM3). As a result, surface winds in the tropics are  $\sim 1 \text{ m s}^{-1}$  too strong. Excess winds cause excess cooling and depressed SSTs north of the equator. However, south of the equator SST is erroneously high due to the presence of additional warming effects. The region of highest SST bias is close to southern Africa near the mean latitude of the Angola–Benguela Front (ABF). Comparison of CCSM4 to ocean simulations of various resolutions suggests that insufficient horizontal resolution leads to the insufficient northward transport of cool water along this coast and an erroneous southward stretching of the ABF. A similar problem arises in the coupled model if the atmospheric component produces alongshore winds that are too weak. Erroneously warm coastal SSTs spread westward through a combination of advection and positive air–sea feedback involving marine stratocumulus clouds.

This study thus highlights three aspects to improve to reduce bias in coupled simulations of the tropical Atlantic: 1) large-scale atmospheric pressure fields; 2) the parameterization of stratocumulus clouds; and 3) the processes, including winds and ocean model resolution, that lead to errors in seasonal SST along southwestern Africa. Improvements of the latter require horizontal resolution much finer than the  $1^\circ$  currently used in many climate models.

### 1. Introduction

Because of its proximity to land and the presence of coupled interaction processes, the seasonal climate of the tropical Atlantic Ocean is notoriously difficult to simulate accurately in coupled models (Zeng et al. 1996; Davey et al. 2002; Deser et al. 2006; Chang et al. 2007; Richter and Xie 2008). Several recent studies, including those referenced above, have linked the ultimate causes of the persistent model biases to problems in simulating

winds and clouds by the atmospheric model component. This paper revisits the problem of biases in coupled simulations of the tropical Atlantic through examination of the Community Climate System Model, version 4 (CCSM4; Gent et al. 2011), a coupled climate model simultaneously simulating the earth's atmosphere, ocean, land surface, and sea ice processes.

The predominant feature of the seasonal cycle of the tropical Atlantic is the seasonal meridional shift of the zonally oriented intertropical convergence zone (ITCZ), which defines the boundary between the southeasterly and northeasterly trade wind systems. As the ITCZ shifts northward in northern summer from its annual mean latitude a few degrees north of the equator, the zonal winds along the equator intensify, increasing the zonal tilt of the oceanic thermocline and bringing cool water into the mixed layer of the eastern equatorial ocean (e.g., Xie and Carton 2004). This northward shift reduces rainfall into the Amazon and Congo basins, reducing the

---

\* The National Center for Atmospheric Research is sponsored by the National Science Foundation.

---

*Corresponding author address:* Semyon A. Grodsky, Department of Atmospheric and Oceanic Science, University of Maryland, College Park, Computer and Space Science Building, Room 2409, College Park, MD 20742.  
E-mail: senya@atmos.umd.edu

discharge of those Southern Hemisphere rivers and enhancing rainfall over Northern Hemisphere river basins, such as the Orinoco, and over the northern tropical ocean. The northward migration of the ITCZ off the west coast of Africa contributes to the sea surface temperature (SST) increase in boreal spring by reducing wind speeds and suppressing evaporation. During this period, the westerly monsoon flow is expanded farther westward and moisture transport onto the continent is enhanced, increasing Sahel rainfall (Grodsky et al. 2003; Hagos and Cook 2009). Rainfall affects sea surface salinity (SSS), which in turn affects SST through its impact on the upper-ocean stratification and barrier layers. These impacts have been found in uncoupled and coupled models (Carton 1991; Breugem et al. 2008). Observational analyses of Pailler et al. (1999), Foltz and McPhaden (2009), and Liu et al. (2009) have also suggested that salinity and barrier layers are important for the climate of the tropical Atlantic.

The northward shift of the ITCZ also leads to a seasonal strengthening of the alongshore winds off southwest subtropical Africa. A low-level atmospheric jet along the Benguela coast is driven by the South Atlantic subtropical high pressure system, with topographic enhancement of winds west of the Namibian highland (Nicholson 2010). This coastal wind jet drives local upwelling as well as the coastal branch of the equatorward Benguela Current, causing equatorward advection of cool Southern Hemisphere water (e.g., Boyer et al. 2000; Colberg and Reason 2006; Rouault et al. 2007). The Benguela Current meets the warm southward-flowing Angola Current at around 17°S, and thus shifts in the Angola–Benguela Front (ABF) position are a cause of large ocean temperature anomalies. The reduced SSTs associated with intensified upwelling have the effect of expanding the area of the eastern ocean covered by a low-lying stratus cloud deck and thus reducing net surface solar radiation (Mechoso et al. 1995; Cronin et al. 2006; Zuidema et al. 2009). In addition to the direct radiation effect, stratus clouds impact vertical motions in the atmosphere. Long-wave cooling from the cloud tops is balanced by adiabatic warming, that is, subsidence. The subsidence leads to near-surface divergence and thus counterclockwise circulation in the Southern Hemisphere, that is, to southerlies along the coast (Nigam 1997). This suggests that a reduction in stratocumulus cover produces erroneous northerlies along the coast, which has the effect of raising SST (by attenuating coastal upwelling) and further reducing cloud cover.

As the seasons progress toward northern winter, the trade wind systems shift southward (toward the warmer hemisphere) and equatorial winds reduce in strength along with a reduction in the zonal SST gradient along

the equator. It is evident from this description that the processes maintaining the seasonal cycle of climate in the tropical Atlantic involve intimate interactions between ocean and atmosphere. Thus, a meridional displacement of the ITCZ and the trade wind systems is linked through wind-driven evaporation effects to a shift in the interhemispheric gradient of SST. Such meridional shifts in both are known to occur every few years [the “meridional” or “dipole” mode, e.g., Xie and Carton (2004)]. Likewise, changes in the strength of the zonal winds and the zonal SST gradient along the equator occur from year to year in a way that is reminiscent of the kinematics and dynamics of ENSO. Indeed, Chang et al. (2007) point out that the existence of these coupled feedback processes may explain why the patterns of SST, wind, and precipitation bias are quite similar from one coupled model to the next, even though careful examination shows that the processes causing these biases may be quite different.

This paper follows examinations of bias in the earlier of the model, CCSM3 (described in Collins et al. 2006a). For example, in CCSM3, both Large and Danabasoglu (2006) and Chang et al. (2007) pointed out that major atmospheric pressure centers and all global-scale surface wind systems are stronger than observed. In the northern tropics, this excess wind forcing results in excess surface heat loss. Despite the excess winds, the SST in the southeastern tropics is too warm. In CCSM3, the SST warm bias in the southeast has been attributed to the remote impact of erroneously weak zonal surface winds along the equator because of a deficit of rainfall over the Amazon basin (Chang et al. 2007, 2008; Richter and Xie 2008), which is in turn affected by remote forcing from the Pacific (Tozuka et al. 2011). This wind–precipitation bias was also shown to be present in the atmospheric model component, the Community Atmosphere Model, version 3 (CAM3), when forced with observed SST as a surface boundary condition. In the ocean, the resulting equatorial zonal wind bias leads to an erroneous deepening of the equatorial thermocline and warming of the cold tongue in the eastern equatorial zone [this bias is common to most of nonflux-corrected coupled simulations of the earlier generation (Davey et al. 2002)]. Predictably, this warm SST bias in the eastern equatorial zone is reduced if the model equatorial winds are strengthened (Richter et al. 2012; Wahl et al. 2011).

The warm SST bias in CCSM3 and many other models extends from the equatorial zone into the tropical southeastern basin, where it is stronger and more persistent (Stockdale et al. 2006; Chang et al. 2007; Huang and Hu 2007). There erroneously warm SSTs result, in part, from the southward transport of the erroneously warm

equatorial water by the Angola Current (Florenchie et al. 2003; Richter et al. 2010). The semiannual downwelling Kelvin waves produced by seasonal wind changes warm the SST along the southwestern coast of Africa in austral fall and early austral spring [see, e.g., Fig. 8a in Lübbecke et al. (2010)]. Because the second baroclinic mode is dominant and thus the width of the current is 40–60 km (e.g., Illig et al. 2004), high resolution will likely prove necessary to resolve the coastal currents and thus accurately reproduce the heat advection contribution to the seasonal variation of coastal SSTs there.

The impact of errors in wind-driven ocean currents is also emphasized by Zheng et al. (2011), who have examined systematic warm biases in SST in the analogous coastal region of the southeastern Pacific in 19 coupled models. Although the overlying stratus clouds also observed to be present in this region are underrepresented in those models due to the presence of a warm SST bias, most have too little net surface heat flux to the ocean. This result suggests that warm SST bias in the stratocumulus deck region of the southeastern Pacific is caused by insufficient poleward ocean heat transport. Indeed, in most of these models, upwelling and alongshore advection off Peru is much weaker than observed because of weaker-than-observed alongshore winds. The crucial importance of coastal upwelling on SST bias throughout the entire southeastern tropical basin has been demonstrated by Large and Danabasoglu (2006) in a coupled run, in which Atlantic water temperature and salinity were kept close to observations along the southern African coastal zone.

One curious result discussed by Large and Danabasoglu (2006) is that a warm SST bias may also be present along the Atlantic coast of southern Africa in forced ocean-only simulations. An explanation for why this bias occurs is the fact that there is a strong SST front at the latitude of the boundary between the warm Angola and cold Benguela Current systems (which should be at  $\sim 17.5^{\circ}\text{S}$ ) (Rouault et al. 2007; Veitch et al. 2010). The position of this front is maintained partly by local wind-induced upwelling, and thus local wind errors will cause errors in its position and strength. Also, even if the local winds are correct, the coastal currents must be resolved numerically (Colberg and Reason 2006). Interestingly, results from previous attempts to improve the coupled simulations solely by improving ocean spatial resolution are ambiguous. Toniazzo et al. (2010) have found apparent improvements of SSTs in the dynamically similar Peruvian upwelling region using an eddy-permitting ocean of  $1/3^{\circ}$  resolution and atmosphere of  $1.25^{\circ} \times 5/6^{\circ}$  resolution in the Hadley Centre coupled model. But, B. P. Kirtman (2011, personnel communication) reports a persistent

warm SST bias in the Benguela region using an eddy-resolving  $0.1^{\circ}$ -resolution ocean coupled with a  $0.5^{\circ}$ -resolution CAM3.5 atmosphere.

Another potential source of bias is the impact of errors in the atmospheric hydrologic cycle on ocean stratification through its effects on ocean salinity. In CCSM3 the appearance of excess precipitation in the Southern Hemisphere and the resulting erroneously high Congo River discharge contributes to an excess freshening of the surface ocean by 1.5 psu, erroneous expansion of oceanic barrier layers, and a resulting erroneous warming of SST in the Gulf of Guinea (Breugem et al. 2008). Conversely, north of the equator, reduced rainfall causes erroneous deepening and enhanced entrainment cooling of winter mixed layers. These processes have the effect of cooling the already cold-biased northern tropical SST (Balaguru et al. 2010).

In this study we extend our examination of seasonal bias in CCSM3 to consider its descendent, CCSM4. Our goals are to compare the CCSM4 bias to that in CCSM3 and to explore some previously suggested and some newly proposed mechanisms to explain the presence of the bias. The region of highest SST bias is located close to the coast of southern Africa, near the mean latitude of the Angola–Benguela Front. As pointed out above, many studies emphasize the role of erroneously weak equatorial zonal winds in producing the spurious accumulation of warm water in the Benguela region (e.g., Wahl et al. 2011). This study also considers the Large and Danabasoglu (2006) mechanism involving the oceanic origin of the warm Benguela bias. Comparison of CCSM4 to ocean simulations of various resolutions suggests that insufficient horizontal resolution does lead to insufficient northward transport of cool water along this coast and to erroneous southward stretching of the ABF. A similar problem arises in coupled models if the atmospheric component produces alongshore winds that are too weak. Once this error is present in the coastal zone, the warm bias in SST spreads westward through a combination of advection and positive air–sea feedback involving marine stratocumulus clouds.

## 2. Model and data

The version of CCSM4 used in this study is the  $1^{\circ} \times 1^{\circ}$  twentieth-century run archived as b40.20th.track1.1deg.005. The CCSM4 twentieth-century runs begin in January 1850 and end in December 2005. They are forced by time-varying solar output, greenhouse gas, volcanic, and other aerosol concentrations (Gent et al. 2011). The results were replicated using output from the 1850 fixed forcing experiment. We compare the climatological monthly variability with the observed monthly variability

TABLE 1. Experiments used in this study. ATM = atmosphere; OCN = ocean.

Experiment	Years	Forcing	Resolution (°)
CCSM4	1850–2005 (1980–2005)	Coupled, twentieth-century run with historical gas forcing	1.25 × 1 ATM 1.125 × 0.5 OCN
CAM4/AMIP	1979–2005	SST (Hurrell et al. 2008)	1.25 × 1
CCSM3	1870–1999 (1949–99)	Coupled, Twentieth-Century Climate in Coupled Model (20C3M) run, historical gas forcing	T85 (1.41 × 1) ATM 1.125 × 0.5 OCN
CAM3/AMIP	1950–2001	SST (Hurrell et al. 2008)	T85
POP_0.25	1871–2008  (1980–2008)	20CR version 2 fluxes (Compo et al. 2011).	0.4 × 0.25 (OCN model resolution in tropics)
POP_0.1/NYF	Model year 64	Repeating annual cycle of NYF (Large and Yeager 2009)	0.5 × 0.5 output grid
POP/NYF	Model years 1–10	Repeating annual cycle of NYF (Large and Yeager 2009)	0.1 × 0.1 1.125 × 0.5

computed from observational analyses during the 26-yr period 1980–2005 (or whatever observations are available during the period).

To understand the contributions of individual components of CCSM4, we also examine atmospheric and oceanic components separately in other experiments carried out by National Center for Atmospheric Research (NCAR) (Table 1). The atmosphere component, known as CAM4, employs an improved deep convection scheme relative to the earlier CAM3 (described in Collins et al. 2006b) by inclusion of convective momentum transport and a dilution approximation for the calculation of convective available potential energy (Neale et al. 2008). The model has 26 vertical levels and 1.25° longitude × 1° latitude resolution, which improves on the T85 (approximately 1.41° zonal resolution) of CAM3. The simulation examined here (1979–2005), referred to as the CAM4/Atmospheric Model Intercomparison Project (AMIP) and archived as f40.1979\_amip.track1.1deg.001, differs from CCSM4, in that it is forced by observed monthly SST (described in Hurrell et al. 2008).

The ocean model component of CCSM4 uses Parallel Ocean Program version 2 (POP2) numerics (Danabasoglu et al. 2012). Among other improvements relative to POP1.3 used in CCSM3, POP2 implements a simplified version of the near-boundary eddy flux parameterization of Ferrari et al. (2008), vertically varying isopycnal diffusivity coefficients (Danabasoglu and Marshall 2007), modified anisotropic horizontal viscosity coefficients with much lower magnitudes than in CCSM3 (Jochum et al. 2008), and a modified *K*-profile parameterization with horizontally varying background vertical diffusivity and viscosity coefficients (Jochum 2009). The number of vertical levels has been increased from 40 levels in CCSM3 to 60 levels in CCSM4. The ocean component of CCSM4 is run with a displaced pole grid with an average horizontal resolution of 1.125° longitude × 0.55° latitude in the midlatitudes (similar to the horizontal ocean grid of CCSM3). To explore errors in the ocean model component, we examine the output from an uncoupled ocean run using the same grid but forced by repeating annually the normal year forcing (NYF) fluxes of Large and Yeager (2009). The experiment we examine

TABLE 2. Datasets used to evaluate seasonal bias.

Variable	Years	Description	Resolution (°)
SST	1982–present	Optimal interpolation version 2 (Reynolds et al. 2002)	1 × 1
10-m winds	1999–2009	QuikSCAT (e.g., Liu 2002)	0.5 × 0.5
Wind stress	1999–2007	QuikSCAT (Bentamy et al. 2008)	1 × 1
Wind stress	Climatology	QuikSCAT (Risien and Chelton 2008)	1/4 × 1/4
Shortwave radiation	2002–10	MODIS (Pinker et al. 2009)	1 × 1
LHTFL	1992–2007	IFREMER satellite based (Bentamy et al. 2003, 2008)	1 × 1
Precipitation	1979–2010	Climate Prediction Center Merged Analysis of Precipitation (Xie and Arkin 1997)	2.5 × 2.5
MSLP	1958–2001	40-yr European Centre for Medium-Range Weather Forecasts Re-Analysis (ERA-40) (Uppala et al. 2005)	2.5 × 2.5
SSS	1871–2008 Used data 1980–2008	SODA version 2.2.4 (Carton and Giese 2008; Giese et al. 2010)	0.5 × 0.5

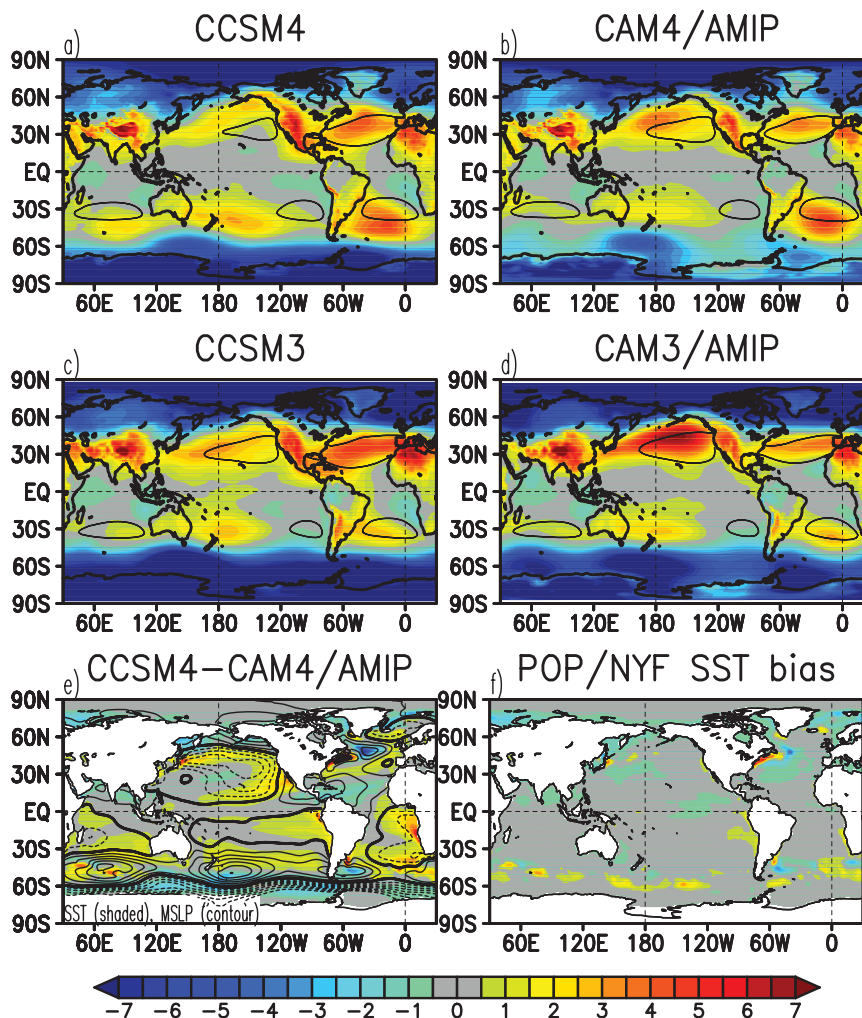


FIG. 1. (a)–(d) Annual mean MSLP bias (mbar) in CCSM and its atmospheric component forced by observed SST (CAM/AMIP). (e), (f) SST bias (shading, °C) in CCSM4 and its ocean model component (POP/NYF). Difference between annual mean MSLP in CCSM4 and CAM4/AMIP is overlaid in (e) as contours (from  $-3.5$  to  $3.5$  mbar at contour intervals =  $0.5$  mbar; positive: solid; negative: dashed; zero: bold). Color bar corresponds to MSLP in (a)–(e) and SST in (e), (f).

is c40.t62x1.verif.01 and is referred to in this paper as POP/NYF.

To explore the impact of changing the ocean model resolution, we examine two additional global ocean simulation experiments, also based on the same POP2 numerics. The first, referred to here as POP\_0.25, has eddy-permitting  $0.4^\circ \times 0.25^\circ$  resolution in the tropics with 40 vertical levels (Carton and Giese 2008). Surface fluxes are provided by the Twentieth-Century Reanalysis Project (20CR) version 2 of Compo et al. (2011). Data from the period 1980–2008 are used to evaluate the monthly climatology from the POP\_0.25 experiment. The second, referred to as POP\_0.1/NYF, has even finer  $0.1^\circ \times 0.1^\circ$  horizontal resolution in the tropics (Maltrud

et al. 2010). The forcing for this simulation is again the NYF fluxes of Large and Yeager (2009). The results shown here are for a single year, year 64. For each experiment, we first monthly average the various atmospheric and oceanic fields, then compute a climatological monthly cycle by averaging successive Januarys, Februarys, etc. Because of our interest in the interactions between atmosphere and ocean, we focus on a few key variables, including SST, SSS, surface winds, and surface heat and freshwater fluxes.

To determine the bias in the various simulations, we compare the model results to a variety of observation-based, or reanalysis-based datasets listed in Table 2. In addition, a detailed comparison is made to observations

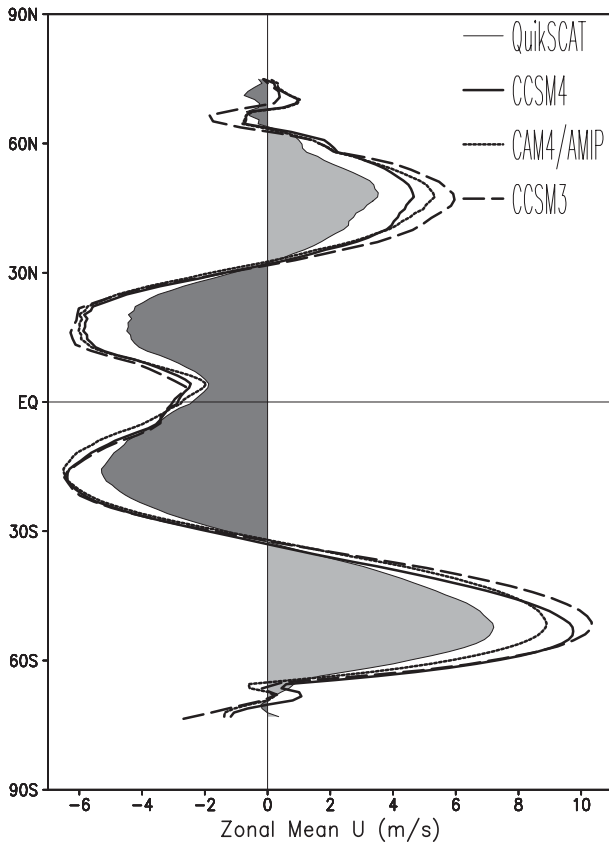


FIG. 2. Annual and zonal mean wind speed  $U$  over the ocean from QuikSCAT (shaded), in CCSM4, in atmospheric component forced by observed SST (CAM4/AMIP), and in CCSM3.

from a fixed mooring at  $10^{\circ}\text{S}$ ,  $10^{\circ}\text{W}$ , which is part of the Prediction and Research Moored Array in the Tropical Atlantic (PIRATA) mooring array and is maintained by a tripartite Brazilian, French, and United States collaborative observational effort (Bourlès et al. 2008). This mooring was first deployed in late 1997 and has been maintained nearly continuously since with a suite of surface flux instruments, as well as in situ temperature and salinity. We use two observation-based estimates of wind stress of Bentamy et al. (2008) and Risien and Chelton (2008), both derived from Quick Scatterometer (QuikSCAT) data. The difference between the two is due to differences in spatial resolution and formulation of the surface drag coefficient in the stress formulation.

### 3. Results

The presentation of the results is organized in the following way. In the first part of this section, we address errors in the large-scale atmospheric circulation and compare them to errors in tropical–subtropical SST. We will find that wind errors are symmetric about the

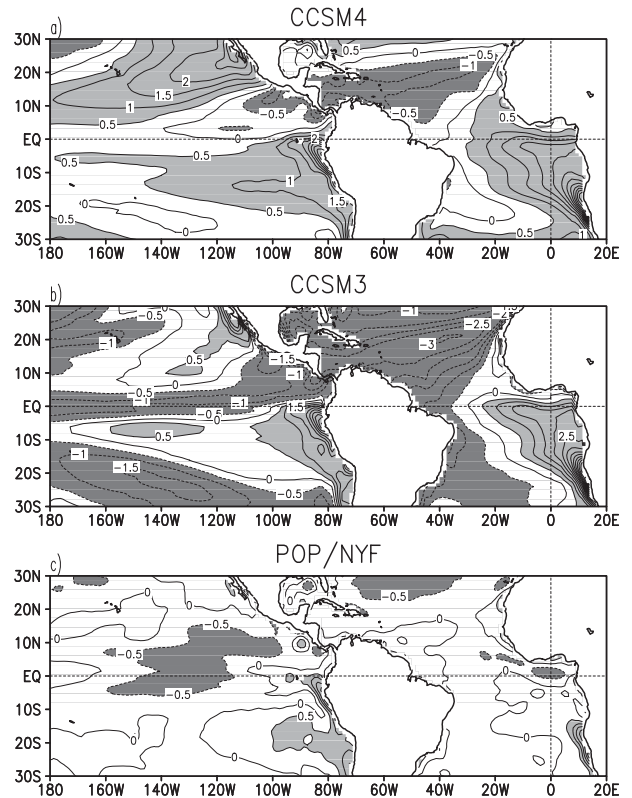


FIG. 3. Annual mean SST bias in (a) CCSM4, (b) CCSM3, and (c) ocean stand-alone component forced by the NYF (POP/NYF).

equator, while the SST errors have an antisymmetric dipolelike pattern (cold: north, warm: south). We next examine the reasons for the dipolelike pattern of SST errors and its link to deficiencies in the atmospheric and oceanic components of the coupled model.

#### a. Gross features

Latitude bands of excessive subtropical mean sea level pressure (MSLP) encircle the globe in both hemispheres in CCSM4 (Fig. 1). This time-mean excess is larger in the Atlantic sector than the Pacific and Indian sectors, and there it exceeds 4–5 mbar (Fig. 1a). We can show that the source of this error is within the atmospheric module, CAM4, because the error is also apparent when SST is replaced with observed climatological SST (CAM4/AMIP; Fig. 1b). This error is even more evident in the previous generation models: CCSM3 and CAM3 (Figs. 1c,d).

One possible explanation for the reduction in time-mean MSLP error between CAM3 and CAM4 is that it is due to improvements to the convection scheme, which in turn affect the Hadley circulation and thus the subtropical surface high pressure systems (Neale et al. 2008). If so, the new convection scheme has different impacts on

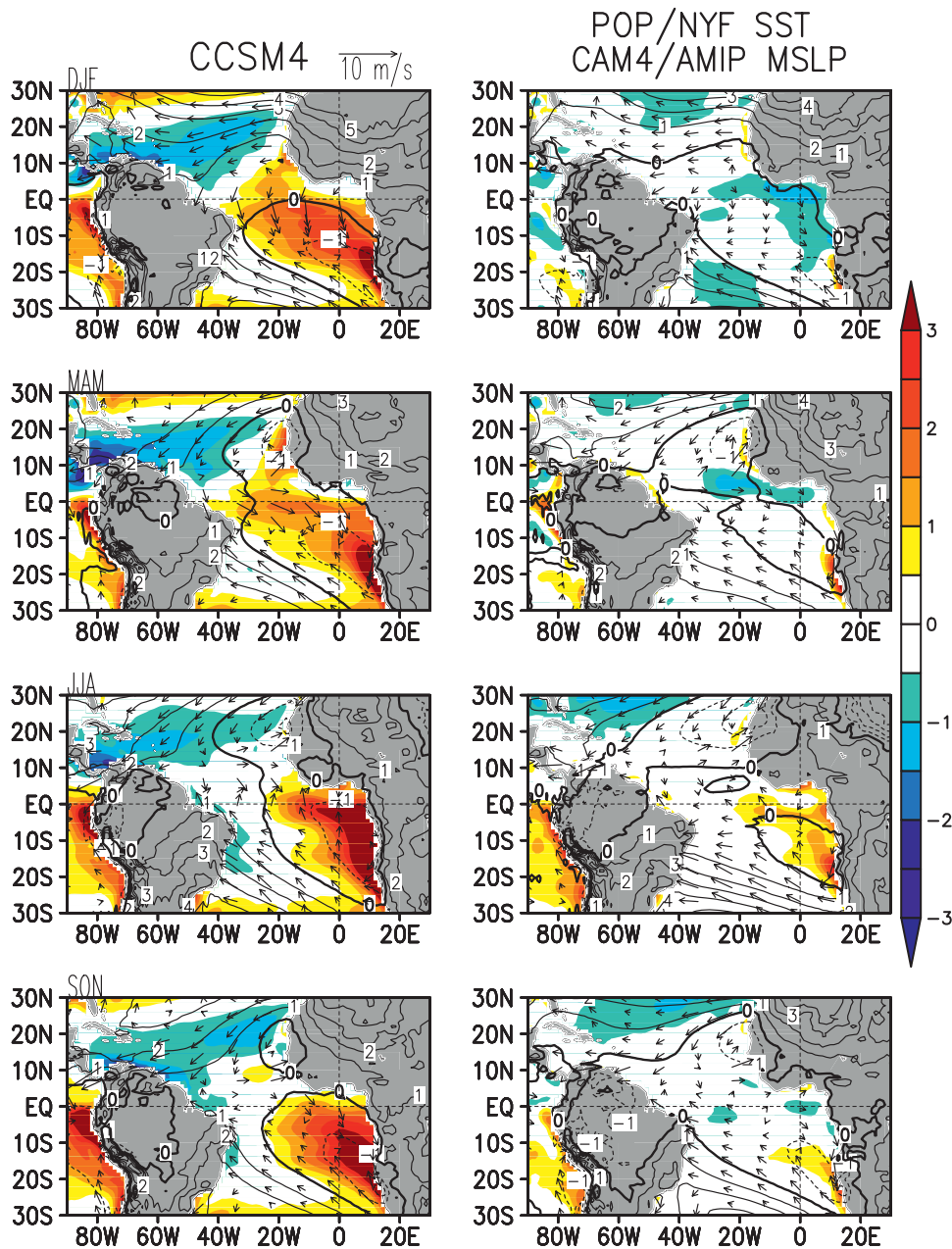


FIG. 4. Bias in SST ( $^{\circ}\text{C}$ , shading) and MSLP (mbar, contours) during (top to bottom) four seasons. (left) CCSM4 data. (right) Data from two independent runs: SST is from a stand-alone ocean model forced by NYF (POP/NYF) and MSLP is from a stand-alone atmospheric model forced by observed SST (CAM4/AMIP). Arrows are the surface wind bias in (left) CCSM4 and (right) CAM4/AMIP.

MSLP in the Northern and Southern Hemispheres: MSLP bias decreases in North Atlantic sector (cf. Figs. 1a,c) as well as the North Pacific sector. However, the bias increases noticeably in the South Atlantic.

The impact of the air–sea coupling on the MSLP bias is evident in comparing CCSM4 and CAM4/AMIP (Fig. 1e). The high MSLP bias in CAM4/AMIP in the northern Atlantic is made worse in CCSM4 due to the

effects of a cold SST bias centered at  $50^{\circ}\text{N}$ ,  $40^{\circ}\text{W}$  (Figs. 1a,b,e). This cold SST bias, in turn, is due to a southward displacement of the Gulf Stream extension, also evident in the POP/NYF ocean-only simulation (Fig. 1f) (Danabasoglu et al. 2012). Farther south SSTs with a cold bias stretch across the northern tropical Atlantic and northeastern tropical Pacific, and are collocated with a positive MSLP difference between the two models

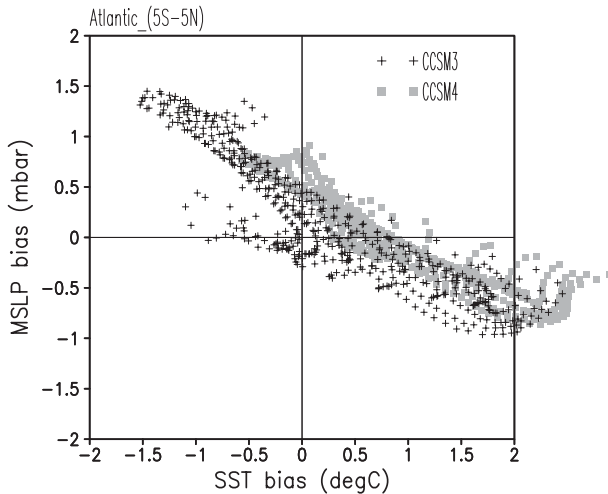


FIG. 5. Scatter diagram of annual mean biases in MSLP and SST over the equatorial Atlantic Ocean ( $5^{\circ}\text{S}$ – $5^{\circ}\text{N}$ ). Each symbol represents gridpoint value.

( $\Delta\text{MSLP} = \text{CCSM4}/\text{CAM4}/\text{AMIP}$ ), while SSTs with a warm bias in the southeastern tropical and southern subtropical Atlantic are collocated with negative  $\Delta\text{MSLP}$  (Fig. 1e). This reduction in MSLP in CCSM4 explains why the MSLP bias is less in the Southern Hemisphere than in the Northern Hemisphere. Incidentally, the MSLP bias is also reduced in the North Pacific (Figs. 1a,b), where air–sea coupling above erroneously cold SST in the Bering Sea and Aleutian Basin and too-warm SST along the Kuroshio Extension appears to produce a response in MSLP that counteracts the original CAM4/AMIP MSLP bias (Figs. 1e,b). Over the equatorial South America, a minor negative MSLP bias in CAM4/AMIP is reduced in CCSM4 (Figs. 1a,b). This reduction may be explained by remote impacts from the eastern tropical Pacific, where the warm SST (Fig. 1e) produces an El Niño–like perturbation of the Walker cell, thus increasing subsidence and air pressure over the equatorial South America.

A consequence of the erroneously high subtropical high pressure systems in CCSM3 and CCSM4 is to produce erroneously strong surface westerlies in mid-latitude (wind speed is too strong by  $\sim 3 \text{ m s}^{-1}$ ) and easterly surface trade winds in the subtropics and tropics (Fig. 2). In turn, these erroneously strong winds can be expected to produce excess evaporation and mixing, giving rise, all other things being equal, to erroneously cool SST. MSLP error in the southeastern tropics, a region where sea level pressure is normally low, is negative (this is also evident in CAM4/AMIP).

Now we focus on the tropical Atlantic sector. Despite that trade winds in CCSM4 are too intense in both hemispheres, errors in annual mean SST are hemispherically asymmetric (Fig. 3a). In the northwestern tropics, SST is

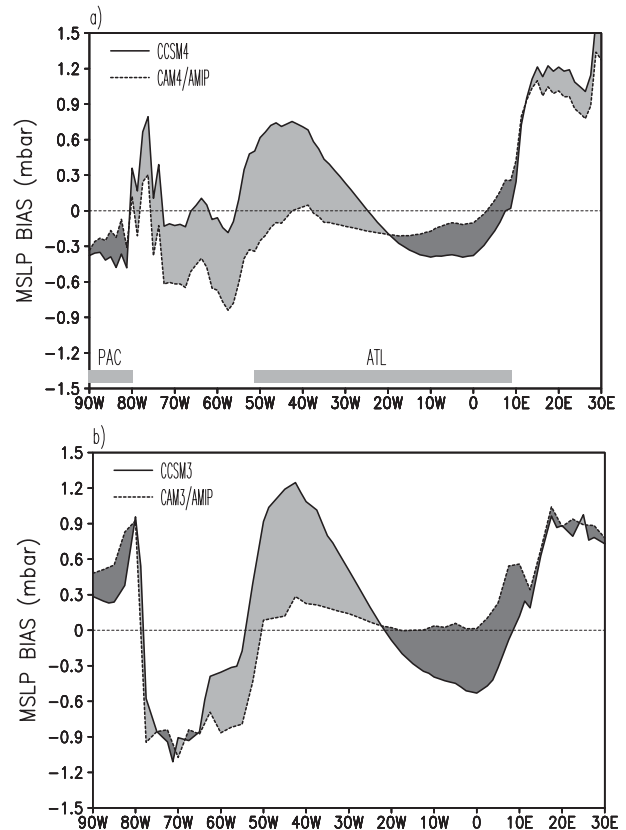


FIG. 6. Annual mean MSLP bias in the  $5^{\circ}\text{S}$ – $5^{\circ}\text{N}$  belt in (solid) CCSM and (dashed) CAM4/AMIP. Difference between the two is shaded. Results of (top) version 4 and (bottom) version 3. Ocean is marked with gray bar in (a).

too cool by  $1^{\circ}\text{C}$ , an error consistent with the effects of  $10 \text{ W m}^{-2}$  excess wind-induced latent heat loss (not shown). The SST is too cold by  $0.5^{\circ}\text{C}$  in the southwestern tropics (Fig. 3a). In contrast, in the southeastern tropics the SST is too warm, growing to  $>5^{\circ}\text{C}$  close to the coast (Fig. 2). This bias is even larger and extends farther westward than that present in CCSM3 due to a global reduction in the net surface heat loss by the ocean (Gent et al. 2011). Conversely, the regions of cold SST bias in CCSM4 are reduced (Figs. 3a,b).

To explore the origin of this complex pattern of SST error in CCSM4, we compare it to the SST error in the CCSM4 ocean model component when forced with representative observed surface forcing (Fig. 3c). The latter also has an SST error of a couple of degrees, mainly near the southern African coast (Figs. 3c,4). This observation suggests that the ocean component and its response to surface forcing may contribute to the initiation of SST errors close to the coast, which may then grow westward.

The seasonal timing of SST errors along the southern African coast is such that they grow in boreal spring and peak in boreal summer in both CCSM4 and in

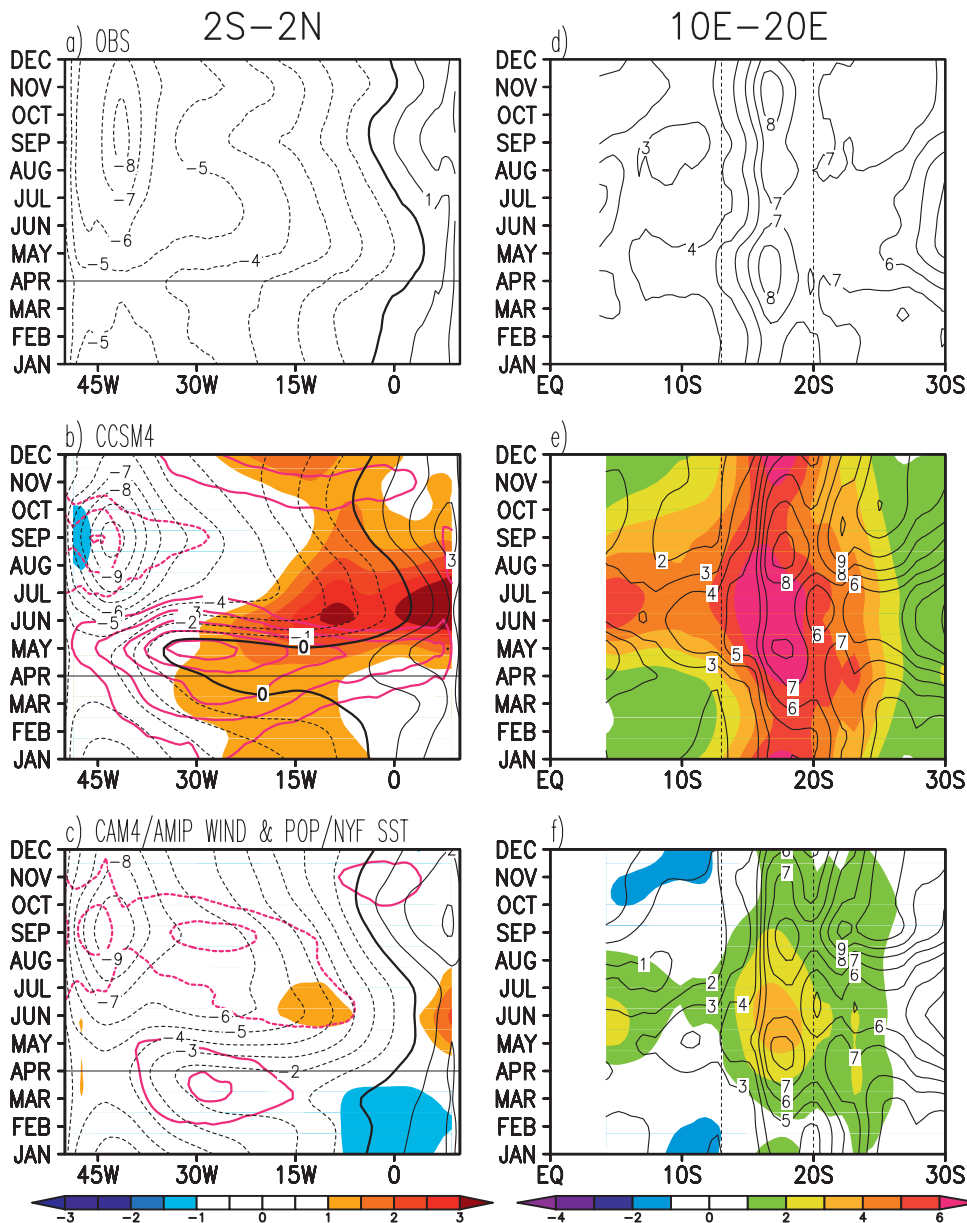


FIG. 7. Observed (a) zonal wind along the equator and (d) meridional wind along the western coast of southern Africa (contour interval is  $1 \text{ m s}^{-1}$ ). (b),(e) CCSM4 SST bias (shading), and winds (black contours). Zonal wind bias is shown for the equatorial zonal winds only (red contours; negative: dashed and positive: solid; contour interval is  $1 \text{ m s}^{-1}$ ; 0 contour is not shown). (c),(f) As in (b),(e) but for CAM4/AMIP winds and POP/NYF SST.

POP/NYF. But in CCSM4 the warm bias is greater and the region of the southeastern tropics biased warm extends considerably farther westward than the corresponding region in POP/NYF (Fig. 4). One possible explanation for this increase in the spatial extent and magnitude of the bias is that it results from positive feedback between the processes involved in the formation of marine stratocumulus clouds over cold water and their cloud shading effect reducing the net surface

radiative forcing. The erroneously warm coastal SSTs in turn could be the result of coastal downwelling Kelvin waves (e.g., Lübbecke et al. 2010) generated by erroneously weak equatorial zonal winds (see March–May in Fig. 4). We note that the spurious warming of the eastern ocean expands coincident with the spurious decline of MSLP, both over the erroneously warm water in the southeastern tropical Atlantic (Fig. 4) and along the equator (Fig. 5).

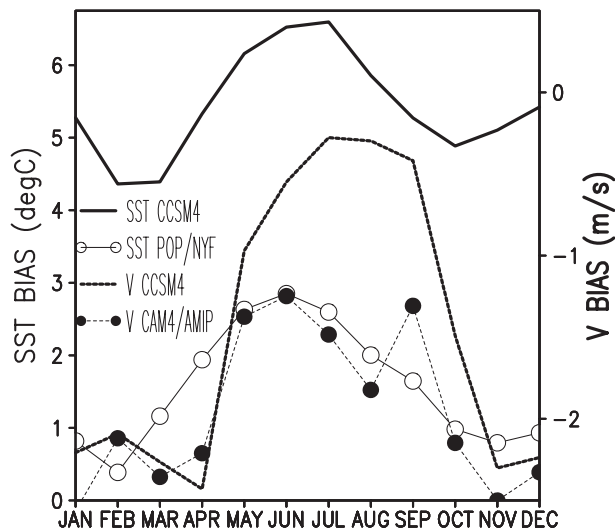


FIG. 8. Seasonal cycle of SST bias and meridional wind ( $V$ ) bias spatially averaged over the ABF region ( $10^{\circ}\text{E}$ –shore,  $20^{\circ}$ – $13^{\circ}\text{S}$ ).

### b. Equatorial zone

The annual mean and seasonal variations of MSLP over the equatorial South America are greatly improved and close to observations in CCSM4 (Figs. 4, 6a). But MSLP is above normal over equatorial Africa in both CCSM4 and CAM4/AMIP. The erroneous eastward gradient of MSLP between the two adjacent landmasses is opposite of the erroneous westward gradient of MSLP over the equatorial Atlantic Ocean, where errors in MSLP closely follow errors in SST (Figs. 4, 5). The annual mean MSLP error over the equatorial Atlantic in CCSM4 is  $+0.6$  mb in the western basin and  $-0.3$  mb in the eastern basin (Fig. 6a), which results in an erroneously weak annual mean eastward gradient of MSLP along the equator (Figs. 5, 6). This error, somewhat reduced from CCSM3, is apparent but not as pronounced in CAM4/AMIP (Fig. 6). A striking difference between CCSM3 and CCSM4 is evident at the eastern edge of the South American continent. In the transition zone between the ocean and continent, the error in CCSM3 annual mean MSLP undergoes a dramatic 2-mb drop, implying a strong erroneous component to the westward pressure gradient force onto the continent. The error in CCSM4 annual mean MSLP undergoes a much smaller decrease, implying a weaker erroneous pressure gradient force, and because it occurs at equatorial latitudes, a weaker downgradient flow onto the continent. The annual mean MSLP over central Africa is erroneously high in both CCSM3 and CCSM4. Both CAM3 and CAM4 also exhibit an erroneous annual mean westward MSLP pressure gradient force—in this case, driving transport from the African continent over the ocean.

In both CCSM3 and CCSM4, the equatorial MSLP biases are worse in the coupled models than in the corresponding atmospheric component, suggesting that some aspect of atmosphere–ocean interactions is acting to enhance the bias (Fig. 6), such as the Bjerknes feedback mechanism (e.g., Richter and Xie 2008), which is suggested by the positive correlation between SST and MSLP biases (Fig. 5). The climatological October zonal wind increase is missing at least in the western equatorial zone (west of  $15^{\circ}\text{W}$ ) in both CAM4/AMIP and CCSM4 (Fig. 7).

Finally, we consider the seasonal evolution of zonal wind and SST bias along the equator. As previously noted, the most striking error in CCSM4 is the erroneous  $5\text{ m s}^{-1}$  weakening of the zonal surface winds in boreal spring (Fig. 7b). This error is noticeably reduced relative to the massive surface wind errors in CCSM3 (Chang et al. 2007), but it is still much stronger than the corresponding errors in CAM4/AMIP (Fig. 7c). The erroneous weakening occurs during the season of northward migration of the southeasterly trade wind system. Thus, the error is partly a reflection of a delay in this migration (cf. Figs. 7a,b), although this does not explain why the winds actually reverse direction. Tentative interpretation of these westerly winds links them to the westerly wind jet that is present in the Atlantic ITCZ (see Grodsky et al. 2003; Hagos and Cook 2009). This westerly jet replaces the southeasterly trades that are normally present along the equator when the core of ITCZ in CCSM4 shifts too far south in March–May. In contrast to the boreal spring weakening, the winds in the western basin in boreal fall are too strong by  $2\text{ m s}^{-1}$  (Fig. 7b). Interestingly, in late boreal summer and early fall, these errors in CAM4/AMIP exceed those of CCSM4, which is attributed to the erroneous eastward gradient of SST (Fig. 7c) and related eastward pressure gradient force counteracting easterly winds.

### c. Conditions along the southern African coast

As noted above, CCSM4 SST is erroneously high along the Benguela region of the southern African coast from  $20^{\circ}$  to  $13^{\circ}\text{S}$  (Figs. 4, 7e). Within approximately  $10^{\circ}$  of the coast and east of  $10^{\circ}\text{E}$ , the bias in CCSM4 SST varies seasonally by approximately  $2^{\circ}\text{C}$  and reaches a maximum ( $>5^{\circ}\text{C}$ ) in austral winter (Fig. 8). The SST bias in POP/NYF has a similar  $\sim 2^{\circ}\text{C}$  seasonal amplitude and seasonal timing (although its annual mean value is several degrees lower), consistent with the idea of an oceanographic origin to this seasonal bias.

In CCSM4 the coastal wind bias is northerly throughout the year (in contrast to the strengthened southeasterly trade winds throughout much of the basin), which causes a reduction in coastal upwelling. However, the

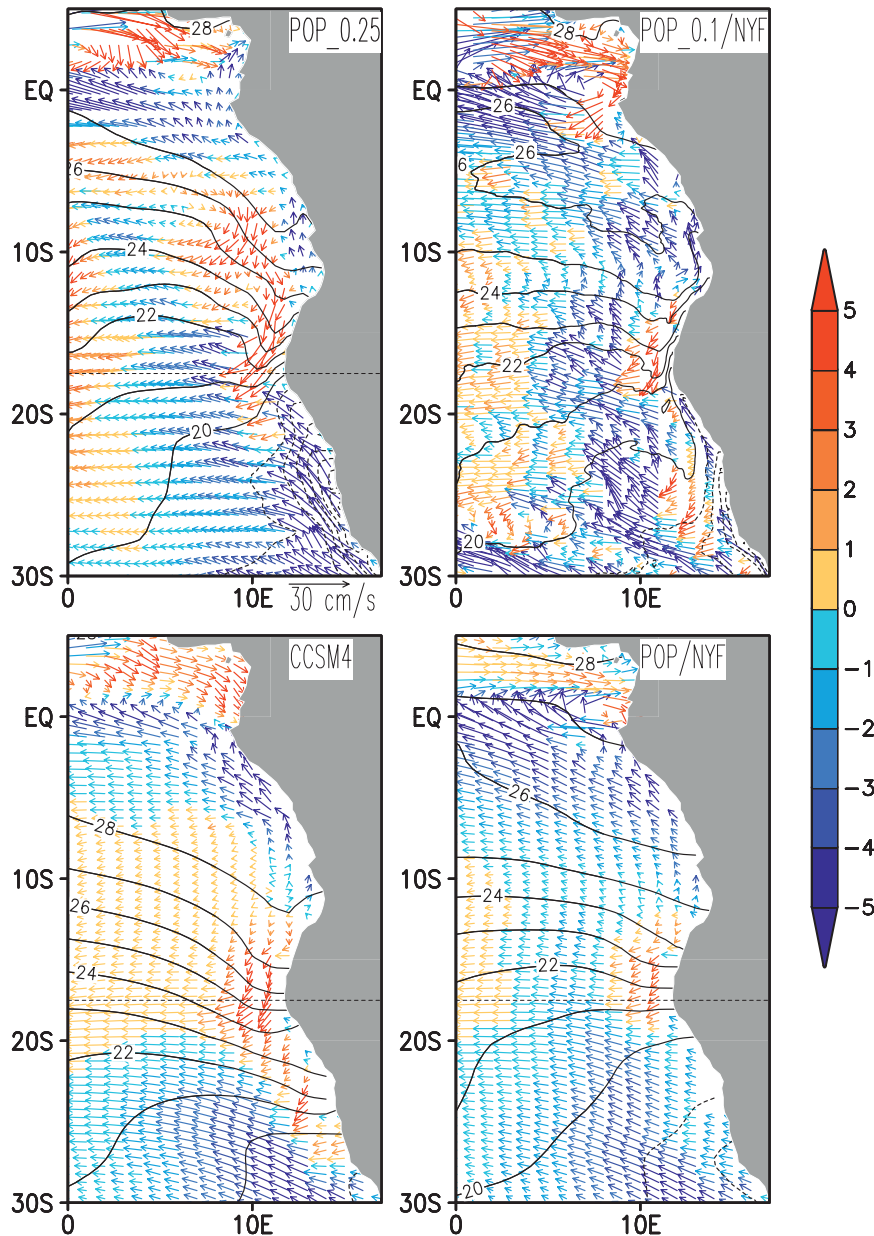


FIG. 9. Annual mean surface currents (arrows) and SST (contours, CINT = 1°C) in (a) POP\_0.25, (b) POP\_0.1/NYF, (c) CCSM4, and (d) POP/NYF. Northward (southward) currents are blue (red). Dashed line is SST below 20°C. Horizontal dashed line is the annual mean latitude of the AFB.

annual mean SST bias in CCSM4 exceeds the annual mean SST bias in POP/NYF by a few degrees Celsius (Fig. 8), providing support for the idea of remote influences of changes in the equatorial winds affecting the SST bias in this region (e.g., Richter et al. 2010, 2012). We also note that the seasonal bias in coastal winds in CCSM4 lags the seasonal bias in the SST bias by approximately one month. Moreover, the warm SST bias of austral spring weakens in austral summer, just when

the arrival of erroneously weak coastal winds should be causing the SST bias to rise. One possible explanation is that at least a part of the warm Benguela SST bias is due to erroneous ocean heat advection.

To explore the possible contribution to Benguela SST bias from erroneous ocean heat advection, we compare the surface currents in CCSM4 to those produced by the three different ocean component models (Table 1). The comparison shows that CCSM4 surface currents closely

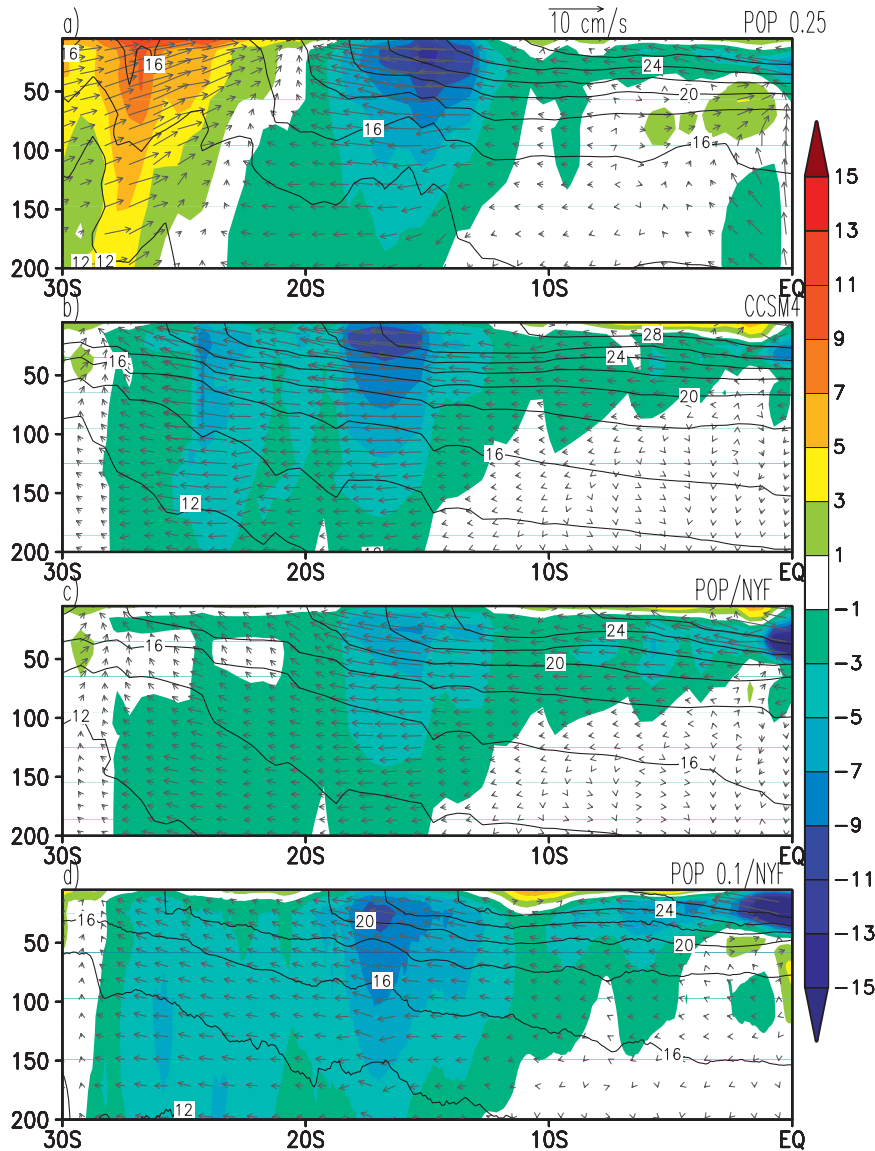


FIG. 10. Annual mean meridional currents (shading), water temperature (contours), and meridional and vertical currents (arrows) averaged  $2^\circ$  off the coast. See Table 1 for description of runs. Arrow scale represents meridional currents. Vertical currents are magnified. Annual mean latitude of the ABF is marked by dashed line.

resemble those of POP/NYF, and in both the coastal Benguela Current is weak and its cold flow does not extend as far north as the climatological position of the Angola–Benguela Front at  $\sim 17^\circ\text{S}$  (Figs. 9b,c).<sup>1</sup> Instead, the Angola Current extends too far south, carrying warm water to coastal regions south of  $20^\circ\text{S}$ . This southward bias in the frontal position explains why the SST bias in CCSM4 is so large near the coast in this range of latitudes.

<sup>1</sup> Coastal currents in CCSM3 are similar to CCSM4 (not shown).

The eddy-resolving POP\_0.1/NYF has a stronger, more coastally trapped Benguela Current (Fig. 9d). But in this experiment as well, ocean advection is acting to warm the coastal ocean too far south of the observed Angola–Benguela frontal position. Of the experiments we examine, only POP\_0.25 has both a reasonable coastal branch of the Benguela Current and has the frontal position at approximately the correct latitude, and thus has greatly reduced the SST bias near the coast (Fig. 9a).

The vertical structure of ocean conditions along the southern African coast confirms our conclusions regarding

the Angola–Benguela frontal position in CCSM4, POP/NYF, and POP\_0.1/NYF (Fig. 10). All three experiments show a strengthening of the southward Angola Current between 15° and 19°S [also evident in the eddy-resolving simulation of Veitch et al. (2010)], and its continuation south of 25°S. In striking contrast, POP\_0.25 shows strong equatorward transport of cool Southern Hemisphere water south of 20°S, extending even farther northward at surface levels. One possible explanation for the erroneous behavior of CCSM4 and POP/NYF is the insufficiency of their ocean horizontal to resolve baroclinic coastal Kelvin waves [which have a width of <60 km at 17°S according to Colberg and Reason (2006); Veitch et al. 2010]. However, the fact that the same error is evident in the high-resolution POP\_0.1/NYF suggests the presence of an error in surface forcing as well.

Comparison of NYF wind stress (Fig. 11b) to satellite-observed wind stress (Fig. 11e) shows that the former has an insufficiently intense low-level Benguela wind jet, which also remains erroneously displaced offshore. It is thus not surprising that the ocean models driven by NYF wind stress have weak coastal currents that are displaced offshore, even if their horizontal resolution is sufficient to resolve coastal currents. In contrast the wind stress used to force POP\_0.25 more closely resembles the satellite-observed winds in this coastal zone (Figs. 11a,f,e). This improved fidelity of the forcing fields explains the presence of a strong coastal jet of the Benguela Current in POP\_0.25 (Figs. 9, 10).

#### d. Surface shortwave radiation

The largest term in net surface heat flux is shortwave radiation. In the southeast CCSM4 and CAM4/AMIP, shortwave radiation is biased high by at least  $20 \text{ W m}^{-2}$  and reaches a maximum of  $60 \text{ W m}^{-2}$  in austral winter and spring (when seasonal SST is cool) due to a lack of shallow stratocumulus clouds (Fig. 12). The bias has actually increased relative to CCSM3, particularly in the eastern ocean boundary regions (see Fig. 2 in Bates et al. 2011, manuscript submitted to *J. Climate*) due to the increase in warm SST bias (Figs. 3a,b) and consequent reduction in cloud cover.

The regional excess of shortwave radiation is compensated for in part by an excess of latent heat loss due to erroneously strong southeasterly trade winds (Fig. 2). These biases are evident in a comparison of CCSM4 surface downward shortwave radiation and latent heat loss (Figs. 13, 14) with moored observations at 10°S, 10°W. At this location, CCSM4 downward shortwave radiation error reaches a maximum of  $60 \text{ W m}^{-2}$  in August, but the annual mean CCSM4 shortwave error of  $+33 \text{ W m}^{-2}$  is almost compensated for by the annual mean latent heat loss error of  $+30 \text{ W m}^{-2}$  [see Zheng

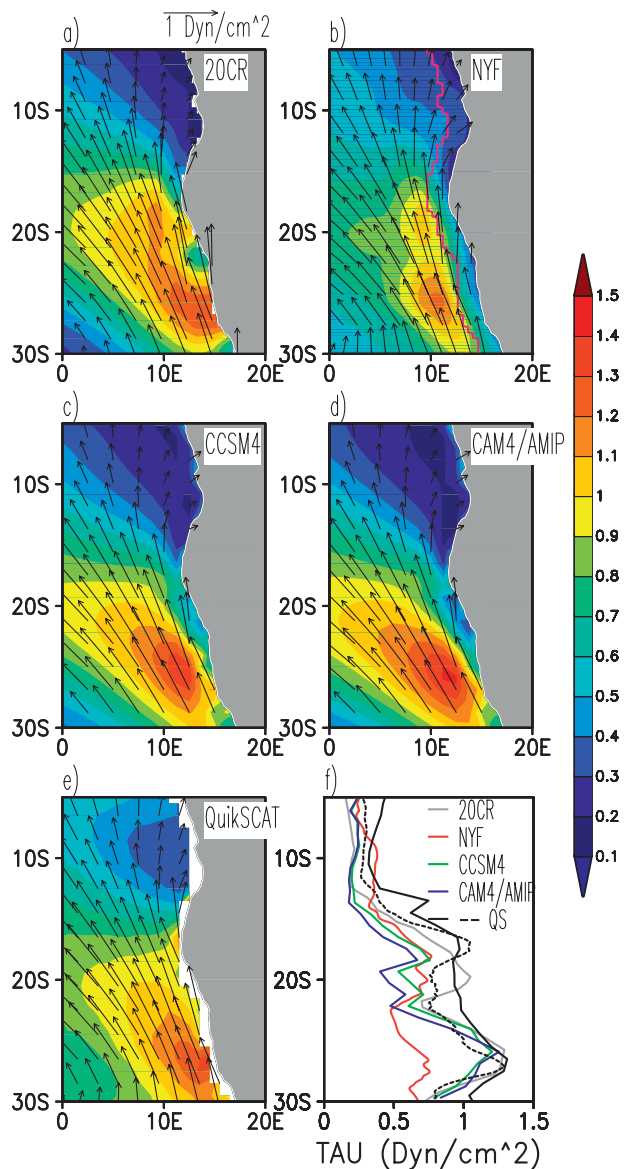


FIG. 11. Annual mean wind stress (arrows) and wind stress magnitude (shading) in the Benguela region. (f) Wind stress magnitude averaged  $2^\circ$  off the coast [red line in (b)]. Two analyses of QuikSCAT wind stress are shown: (solid) Bentamy et al. (2008) and (dashed) Risien and Chelton (2008).

et al. (2011) for similar comparisons in the southeastern Pacific stratocumulus deck region]. On and south of the equator, CCSM4 surface downward shortwave radiation is erroneously low (Fig. 12) due to the erroneous southward displacement of the ITCZ (Figs. 15a,b).

#### e. Precipitation and salinity

The erroneous southward displacement of the ITCZ in CCSM4 leads, on the eastern side of the basin, to excess Congo River discharge by at least a factor of 2

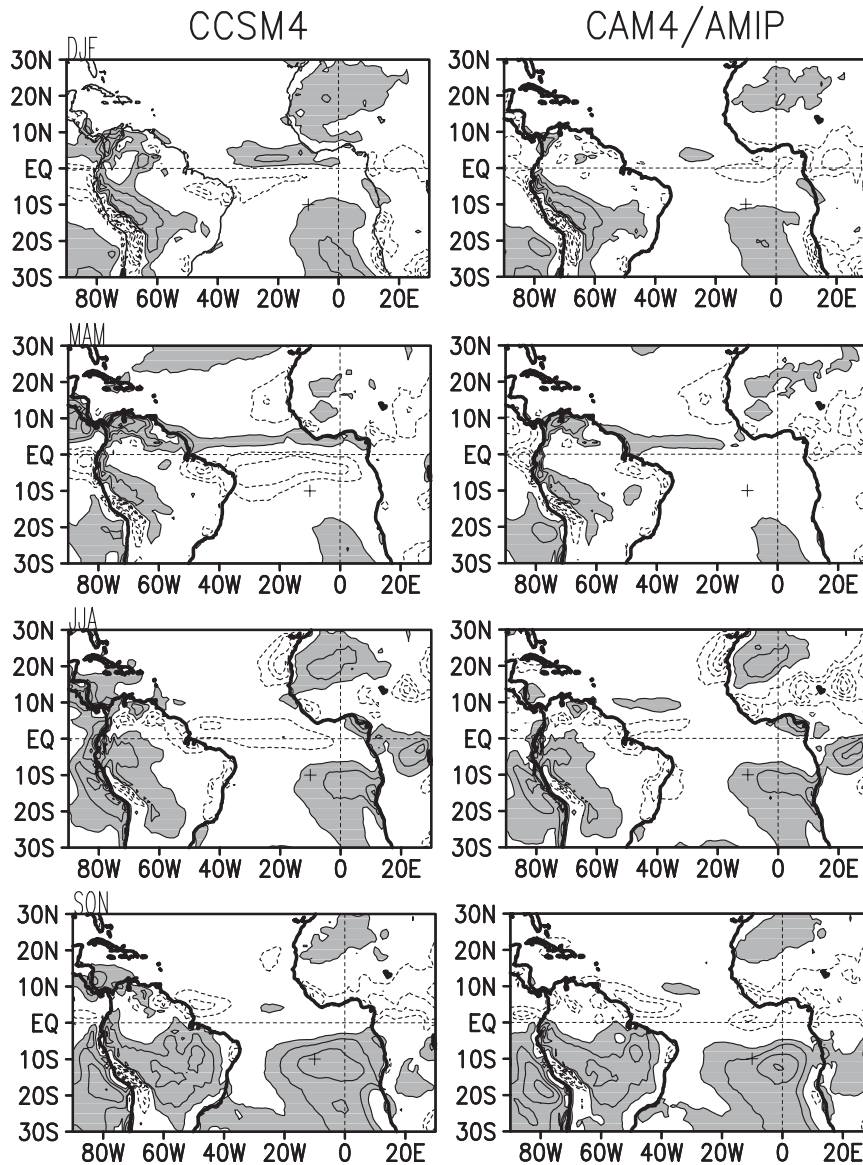


FIG. 12. Seasonal bias in downwelling surface short wave radiation in (left) CCSM4 and (right) CAM4/AMIP with contour interval =  $20 \text{ W m}^{-2}$ . Positive (negative) values are shown by solid (dashed). Zero contour is not shown. The PIRATA mooring location at  $10^{\circ}\text{S}$ ,  $10^{\circ}\text{W}$  is marked by +.

(Fig. 16). Interestingly, on the western side of the basin, CCSM3 had insufficient precipitation over the Amazon basin and thus insufficient Amazon River discharge (Fig. 16c). In CCSM4 precipitation over the Amazon basin is more realistic, and thus Amazon River discharge more closely resembles observations, but it is still too low (Fig. 16b). These biases in precipitation and river discharge on the eastern and western sides of the basin contribute to a CCSM4 SSS fresh bias in the eastern basin and likely contribute to the warm bias in SST by inhibiting vertical mixing. This freshwater bias

is advected around the southern subtropical gyre and results in a lowering of the south subtropical salinity maximum by 1 psu. That, in turn, might indirectly impact the tropical–subtropical water exchange by inhibiting subduction in the southern subtropics.

#### 4. Summary

This paper revisits biases in coupled simulations of the tropical/subtropical Atlantic sector based on analysis of an approximately 25-yr-long sample of the

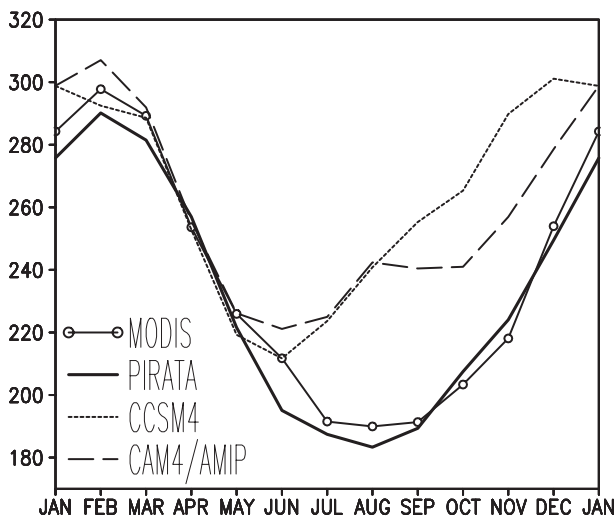


FIG. 13. Seasonal cycle of downwelling shortwave radiation ( $\text{W m}^{-2}$ ) at  $10^{\circ}\text{S}$ ,  $10^{\circ}\text{W}$  from Moderate Resolution Imaging Spectroradiometer (MODIS) satellite retrievals, observed at the PIRATA mooring and simulated by CCSM4 and CAM4/AMIP.

twentieth-century CCSM4 run (1980–2005). Our emphasis is on exploring the causes of biases in basin-scale surface winds and in the coastal circulation in the southeastern boundary and their consequences for producing biases in SST. Here we identify five factors that seem to be important, many of which have been previously identified as problems in other regions or models.

- 1) Excessive trade winds—Like its predecessor model, CCSM3, the CAM4 atmospheric component of CCSM4 has abnormally intense surface subtropical high pressure systems and abnormally low polar low pressure systems (each by a few millibars), and these biases in MSLP cause correspondingly excess surface winds. In the tropics and subtropics, the trade wind winds are  $1\text{--}2 \text{ m s}^{-1}$  too strong in both CAM4/AMIP and CCSM4. As a consequence, latent heat loss is too large.
- 2) Weak equatorial zonal winds—Despite the presence of excessive trade winds off the equator in both hemispheres, SST in the southeast has a warm bias. A contributing factor to this warm bias along the southern African coastal zone is the erroneously weak equatorial winds, which contribute a downwelling Kelvin wave, thus advecting warm water southward to deepen the thermocline along this coast.
- 3) Insufficient coastal currents/upwelling—By comparing the results of CCSM4 with a suite of ocean simulations with different spatial resolutions using different wind forcings, we find that the warm bias evident along the coast of southern Africa is also

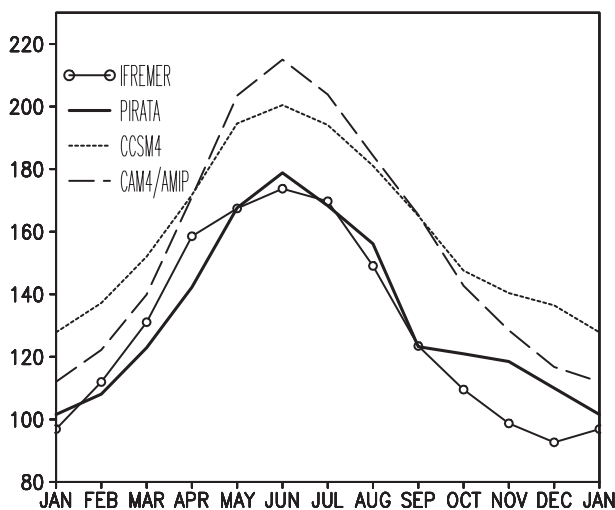


FIG. 14. Seasonal cycle of latent heat flux ( $\text{LHTFL}$ ,  $\text{W m}^{-2}$ ) at  $10^{\circ}\text{S}$ ,  $10^{\circ}\text{W}$  from Institut Français de Recherche pour l'exploitation de la Mer (IFREMER) satellite retrievals of Bentamy et al. (2008), from the PIRATA mooring, and simulated by CCSM4 and CAM4/AMIP. Observed LHTFL is calculated from the buoy data using version 3 of the Coupled Ocean–Atmosphere Response Experiment (COARE 3.0) algorithm of Fairall et al. (2003).

- partly a result of insufficient local upwelling. The first is a consequence of horizontal resolution that is insufficient to resolve a fundamental process of coastal dynamics: the baroclinic coastal Kelvin wave. The second is the erroneous weakness of the wind field within  $2^{\circ}$  of the entire coast of southern Africa. The impact of either of these errors (both of which are present in CCSM4) is to allow the warm Angola Current to extend too far south against the opposing flow of the cold Benguela Current. The resulting warm bias of coastal SST may expand westward through coupled air–sea feedbacks, for example, due to its effect on low-level cloud formation.
- 4) Excessive shortwave radiation—Excess radiation is evident in the south stratocumulus region of up to  $60 \text{ W m}^{-2}$ . This excessive shortwave radiation is connected to the problem of insufficient low-level stratocumulus clouds, which in turn is connected to the problem of erroneously high SST.
  - 5) Spurious freshening—Another feedback mechanism involves the effects of excess precipitation in the Southern Hemisphere on surface salinity, and thus indirectly on SST through enhancing vertical stratification and thus reducing entrainment cooling.

It is unclear which of these factors are most important because likely they all are connected to some extent through air–sea coupling. To cut the feedback circle, we suggest first focusing on correcting factor 1: the mean sea

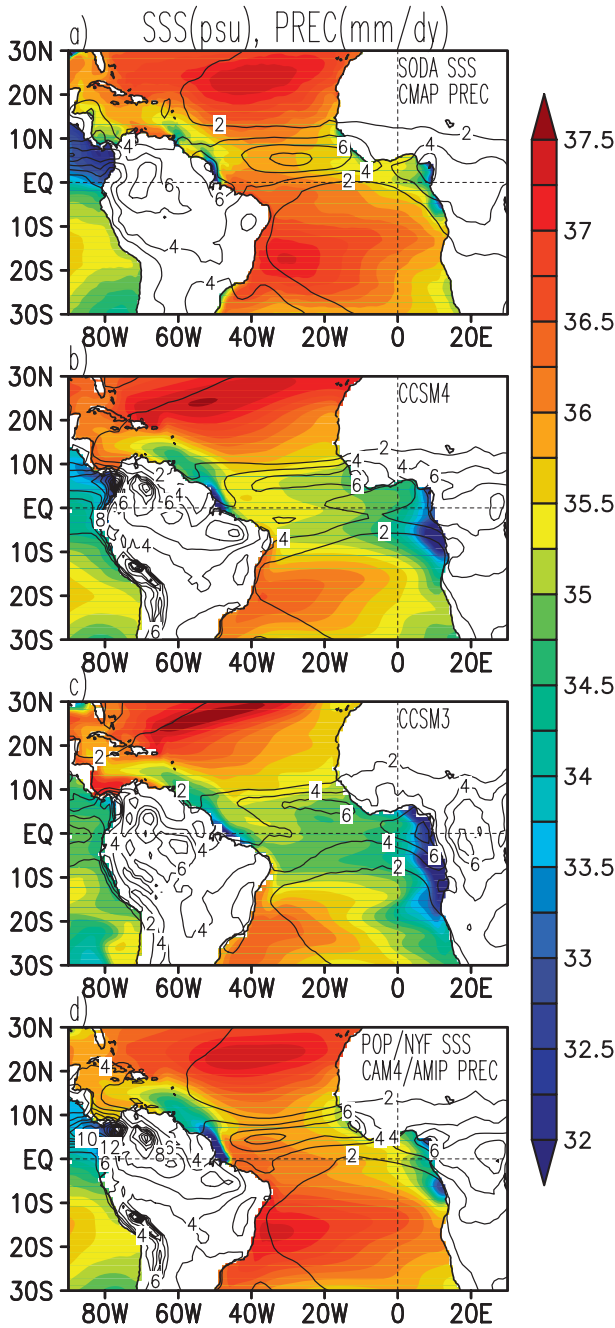


FIG. 15. Annual mean SSS (psu, shading) and precipitation ( $\text{mm day}^{-1}$ , contours): (a) Simple Ocean Data Assimilation (SODA) salinity and CMAP precipitation; (b),(c) CCSM4, CCSM3 SSS, and precipitation; and (d) data from two independent uncoupled runs: POP/NYF SSS and CAM4/AMIP precipitation.

level pressure bias in the atmospheric model component. Correcting this would reduce the cold SST bias in the north tropics, decrease the erroneous southward displacement of the ITCZ, and thus strengthen the equatorial easterly winds (factor 2). Of equal importance,

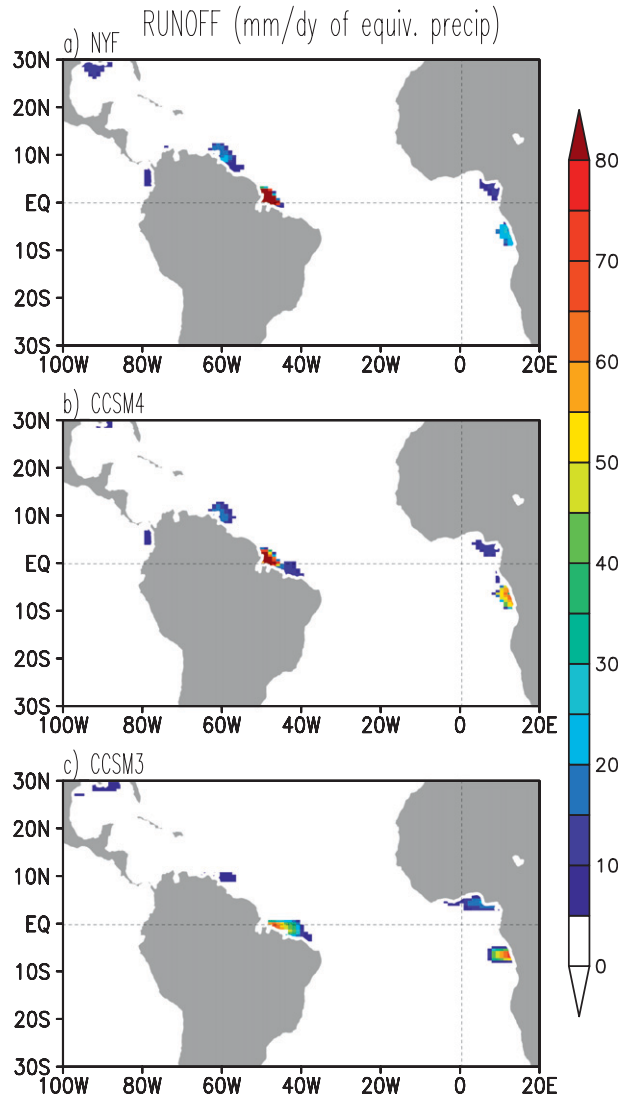


FIG. 16. Annual mean river runoff shown as equivalent surface freshwater flux ( $\text{mm day}^{-1}$ ): (a) NYF of Large and Yeager (2009) (b) CCSM4, and (c) CCSM3.

we suggest improving the stratocumulus cloud parameterization (Madeiros 2011). Errors in the cloud parameterization are apparent in CAM4/AMIP and are amplified through air–sea interactions, as discussed above, leading to massively excess solar radiation in austral winter and spring in CCSM4 (factor 4). Finally, we recommend improving representation of currents and upwelling along the southwestern coast of Africa to maintain the location of the Angola–Benguela SST front (factor 3). Unfortunately, recent experiments by Kirtman et al. (2011) and Patricola et al. (2011) suggest that the simple solution of increasing ocean model horizontal resolution is unlikely to solve this particular problem.

**Acknowledgments.** This research was supported by the NOAA/CPO/CPV (Grant NA08OAR4310878) and NASA ocean programs (Grant NNX09AF34G). Computing resources were provided by the Climate Simulation Laboratory at NCAR's Computational Information Systems Laboratory (CISL), sponsored by the National Science Foundation (NSF) and other agencies. This research was enabled by CISL compute and storage resources. Bluefire, a 4064-processor IBM Power6 resource with a peak of 77 teraflops, provided more than 7.5 million computing hours, the GLADE high-speed disk resources provided 0.4 PB of dedicated disk and CISL's 12-PB HPSS archive provided more than 1 PB of storage in support of this research project. The anonymous reviewers' comments were very helpful and stimulating.

## REFERENCES

- Balaguru, K., P. Chang, and R. Saravanan, cited 2010: Barrier layers in the Atlantic warm pool: Formation and influence on climate. [Available online at <http://www.aoml.noaa.gov/phod/pne/pirata15/karthik.pdf>.]
- Bentamy, A., K. B. Katsaros, A. M. Mestas-Nuñez, W. M. Drennan, E. B. Forde, and H. Roquet, 2003: Satellite estimates of wind speed and latent heat flux over the global oceans. *J. Climate*, **16**, 637–656.
- , L.-H. Ayina, W. Drennan, K. Katsaros, A. M. Mestas-Nuñez, and R. T. Pinker, 2008: 15 years of ocean surface momentum and heat fluxes from remotely sensed observations. *FLUX NEWS*, No. 5, WCRP Working Group on Surface Fluxes, 14–16. [Available online at [sail.msk.ru/newsletter/fluxnews\\_5\\_final.pdf](http://sail.msk.ru/newsletter/fluxnews_5_final.pdf).]
- Bourlès, B., and Coauthors, 2008: The PIRATA program: History, accomplishments, and future directions. *Bull. Amer. Meteor. Soc.*, **89**, 1111–1125.
- Boyer, D., J. Cole, and C. Bartholomae, 2000: Southwestern Africa: Northern Benguela Current region. *Mar. Pollut. Bull.*, **41**, 123–140, doi:10.1016/S0025-326X(00)00106-5.
- Breugem, W. P., P. Chang, C. J. Jang, J. Mignot, and W. Hazeleger, 2008: Barrier layers and tropical Atlantic SST biases in coupled GCMs. *Tellus*, **60A**, 885–897.
- Carton, J. A., 1991: Effect of seasonal surface freshwater flux on sea surface temperature in the tropical Atlantic Ocean. *J. Geophys. Res.*, **96**, 12 593–12 598.
- , and B. S. Giese, 2008: A reanalysis of ocean climate using Simple Ocean Data Assimilation (SODA). *Mon. Wea. Rev.*, **136**, 2999–3017.
- Chang, C.-Y., J. A. Carton, S. A. Grodsky, and S. Nigam, 2007: Seasonal climate of the tropical Atlantic sector in the NCAR Community Climate System Model 3: Error structure and probable causes of errors. *J. Climate*, **20**, 1053–1070.
- , S. Nigam, and J. A. Carton, 2008: Origin of the springtime westerly bias in equatorial Atlantic surface winds in the Community Atmosphere Model version 3 (CAM3) simulation. *J. Climate*, **21**, 4766–4778.
- Colberg, F., and C. J. C. Reason, 2006: A model study of the Angola Benguela frontal zone: Sensitivity to atmospheric forcing. *Geophys. Res. Lett.*, **33**, L19608, doi:10.1029/2006GL027463.
- Collins, W. D., and Coauthors, 2006a: The Community Climate System Model version 3 (CCSM3). *J. Climate*, **19**, 2122–2143.
- , and Coauthors, 2006b: The formulation and atmospheric simulation of the Community Atmosphere Model version 3 (CAM3). *J. Climate*, **19**, 2144–2161.
- Compo, G. P., and Coauthors, 2011: The Twentieth Century Reanalysis Project. *Quart. J. Roy. Meteor. Soc.*, **137**, 1–28.
- Cronin, M. F., N. A. Bond, C. W. Fairall, and R. A. Weller, 2006: Surface cloud forcing in the east Pacific stratus deck/cold tongue/ITCZ complex. *J. Climate*, **19**, 392–409.
- Danabasoglu, G., and J. Marshall, 2007: Effects of vertical variations of thickness diffusivity in an ocean general circulation model. *Ocean Modell.*, **18**, 122–141, doi:10.1016/j.ocemod.2007.03.006.
- , S. Bates, B. P. Briegleb, S. R. Jayne, M. Jochum, W. G. Large, S. Peacock, and S. G. Yeager, 2012: The CCSM4 ocean component. *J. Climate*, **25**, 1361–1389.
- Davey, M., and Coauthors, 2002: STOIC: A study of coupled model climatology and variability in tropical ocean regions. *Climate Dyn.*, **18**, 403–420.
- Deser, C., A. Capotondi, R. Saravanan, and A. Phillips, 2006: Tropical Pacific and Atlantic climate variability in CCSM3. *J. Climate*, **19**, 2451–2481.
- Fairall, C. W., E. F. Bradley, J. E. Hare, A. A. Grachev, and J. B. Edson, 2003: Bulk parameterization of air–sea fluxes: Updates and verification for the COARE algorithm. *J. Climate*, **16**, 571–591.
- Ferrari, R., J. McWilliams, V. Canuto, and M. Dubovikov, 2008: Parameterization of eddy fluxes near oceanic boundaries. *J. Climate*, **21**, 2770–2789.
- Florenchie, P., J. R. E. Lutjeharms, C. J. C. Reason, S. Masson, and M. Rouault, 2003: The source of Benguela Niños in the South Atlantic Ocean. *Geophys. Res. Lett.*, **30**, 1505, doi:10.1029/2003GL017172.
- Foltz, G. R., and M. J. McPhaden, 2009: Impact of barrier layer thickness on SST in the central tropical North Atlantic. *J. Climate*, **22**, 285–299.
- Gent, P. R., and Coauthors, 2011: The Community Climate System Model version 4. *J. Climate*, **24**, 4973–4991.
- Giese, B. S., N. C. Slowey, S. Ray, G. P. Compo, P. D. Sardeshmukh, J. A. Carton, and J. S. Whitaker, 2010: The 1918/19 El Niño. *Bull. Amer. Meteor. Soc.*, **91**, 177–183.
- Grodsky, S. A., J. A. Carton, and S. Nigam, 2003: Near surface westerly wind jet in the Atlantic ITCZ. *Geophys. Res. Lett.*, **30**, 2009, doi:10.1029/2003GL017867.
- Hagos, S. M., and K. H. Cook, 2009: Development of a coupled regional model and its application to the study of interactions between the West African monsoon and the eastern tropical Atlantic Ocean source. *J. Climate*, **22**, 2591–2604.
- Huang, B., and Z.-Z. Hu, 2007: Cloud-SST feedback in southeastern tropical Atlantic anomalous events. *J. Geophys. Res.*, **112**, C03015, doi:10.1029/2006JC003626.
- Hurrell, J. W., J. J. Hack, D. Shea, J. M. Caron, and J. Rosinski, 2008: A new sea surface temperature and sea ice boundary dataset for the Community Atmosphere Model. *J. Climate*, **21**, 5145–5153.
- Illig, S., B. Dewitte, N. Ayoub, Y. du Penhoat, G. Reverdin, P. De Mey, F. Bonjean, and G. S. E. Lagerloef, 2004: Interannual long equatorial waves in the tropical Atlantic from a high-resolution ocean general circulation model experiment in 1981–2000. *J. Geophys. Res.*, **109**, C02022, doi:10.1029/2003JC001771.
- Jochum, M., 2009: Impact of latitudinal variations in vertical diffusivity on climate simulations. *J. Geophys. Res.*, **114**, C01010, doi:10.1029/2008JC005030.

- , G. Danabasoglu, M. Holland, Y.-O. Kwon, and W. G. Large, 2008: Ocean viscosity and climate. *J. Geophys. Res.*, **113**, C06017, doi:10.1029/2007JC004515.
- Kirtman, B. P., and Coauthors, 2011: Impact of ocean model resolution on CCSM climate simulations. *U.S. CLIVAR Variations*, Vol. 9, U.S. CLIVAR Office, Washington, DC, 1–4. [Available online at <http://www.usclivar.org/Newsletter/V9N2.pdf>.]
- Large, W. G., and G. Danabasoglu, 2006: Attribution and impacts of upper-ocean biases in CCSM3. *J. Climate*, **19**, 2325–2346.
- , and S. G. Yeager, 2009: The global climatology of an inter-annually varying air-sea flux data set. *Climate Dyn.*, **33**, 341–364.
- Liu, H., S. A. Grodsky, and J. A. Carton, 2009: Observed sub-seasonal variability of oceanic barrier and compensated layers. *J. Climate*, **22**, 6104–6119.
- Liu, W. T., 2002: Progress in scatterometer application. *J. Oceanogr.*, **58**, 121–136.
- Lübbecke, J. F., C. W. Böning, N. S. Keenlyside, and S.-P. Xie, 2010: On the connection between Benguela and equatorial Atlantic Niños and the role of the South Atlantic anticyclone. *J. Geophys. Res.*, **115**, C09015, doi:10.1029/2009JC005964.
- Madeiros, B., 2011: Comparing the Southern Hemisphere stratocumulus decks in the Community Atmosphere model. *U.S. CLIVAR Variations*, Vol. 9, U.S. CLIVAR Office, Washington, DC, 5–8. [Available online at <http://www.usclivar.org/Newsletter/V9N2.pdf>.]
- Maltrud, M., F. Bryan, and S. Peacock, 2010: Boundary impulse response functions in a century-long eddying global ocean simulation. *Environ. Fluid Mech.*, **10**, 275–295, doi:10.1007/s10652-009-9154-3.
- Mechoso, C. R., and Coauthors, 1995: The seasonal cycle over the tropical Pacific in coupled ocean–atmosphere general circulation models. *Mon. Wea. Rev.*, **123**, 2825–2838.
- Neale, R. B., J. H. Richter, and M. Jochum, 2008: The impact of convection on ENSO: From a delayed oscillator to a series of events. *J. Climate*, **21**, 5904–5924.
- Nicholson, S. E., 2010: A low-level jet along the Benguela coast, an integral part of the Benguela Current ecosystem. *Climatic Change*, **99**, 613–624.
- Nigam, S., 1997: The annual warm to cold phase transition in the eastern equatorial Pacific: Diagnosis of the role of stratus cloud-top cooling source. *J. Climate*, **10**, 2447–2467.
- Pailler, K., B. Bourles, and Y. Gouriou, 1999: The barrier layer in the western tropical Atlantic Ocean. *Geophys. Res. Lett.*, **26**, 2069–2072.
- Patricola, C. M., P. Chang, R. Saravanan, M. Li, and J.-S. Hsieh, 2011: An investigation of the tropical Atlantic bias problem using a high-resolution coupled regional climate model. *U.S. CLIVAR Variations*, Vol. 9, U.S. CLIVAR Office, Washington, DC, 9–12. [Available online at <http://www.usclivar.org/Newsletter/V9N2.pdf>.]
- Pinker, R. T., H. Wang, and S. A. Grodsky, 2009: How good are ocean buoy observations of radiative fluxes? *Geophys. Res. Lett.*, **36**, L10811, doi:10.1029/2009GL037840.
- Reynolds, R. W., N. A. Rayner, T. M. Smith, D. C. Stokes, and W. Wang, 2002: An improved in situ and satellite SST analysis for climate. *J. Climate*, **15**, 1609–1625.
- Richter, I., and S.-P. Xie, 2008: On the origin of equatorial Atlantic biases in coupled general circulation models. *Climate Dyn.*, **31**, 587–598, doi:10.1007/s00382-008-0364-z.
- , S. K. Behera, Y. Masumoto, B. Taguchi, N. Komori, and T. Yamagata, 2010: On the triggering of Benguela Niños: Remote equatorial versus local influences. *Geophys. Res. Lett.*, **37**, L20604, doi:10.1029/2010GL044461.
- , S.-P. Xie, A. T. Wittenberg, and Y. Masumoto, 2012: Tropical Atlantic biases and their relation to surface wind stress and terrestrial precipitation. *Climate Dyn.*, doi:10.1007/s00382-011-1038-9, in press.
- Risien, C. M., and D. B. Chelton, 2008: A global climatology of surface wind and wind stress fields from eight years of QuikSCAT scatterometer data. *J. Phys. Oceanogr.*, **38**, 2379–2413.
- Rouault, M., S. Illig, C. Bartholomae, C. J. C. Reason, and A. Bentamy, 2007: Propagation and origin of warm anomalies in the Angola Benguela upwelling system in 2001. *J. Mar. Syst.*, **68**, 473–488, doi:10.1016/j.jmarsys.2006.11.010.
- Stockdale, T. N., M. A. Balmaseda, and A. Vidard, 2006: Tropical Atlantic SST prediction with coupled ocean–atmosphere GCMs. *J. Climate*, **19**, 6047–6061.
- Toniazzo, T., C. R. Mechoso, L. C. Shaffrey, and J. M. Slingo, 2010: Upper-ocean heat budget and ocean eddy transport in the south-east Pacific in a high-resolution coupled model. *Climate Dyn.*, **35**, 1309–1329, doi:10.1007/s00382-009-0703-8.
- Tozuka, T., T. Doi, T. Miyasaka, N. Keenlyside, and T. Yamagata, 2011: Key factors in simulating the equatorial Atlantic zonal sea surface temperature gradient in a coupled general circulation model. *J. Geophys. Res.*, **116**, C06010, doi:10.1029/2010JC006717.
- Uppala, S. M., and Coauthors, 2005: The ERA-40 Re-Analysis. *Quart. J. Roy. Meteor. Soc.*, **131**, 2961–3012, doi:10.1256/qj.04.176.
- Veitch, J., P. Penven, and F. Shillington, 2010: Modeling equilibrium dynamics of the Benguela Current system. *J. Phys. Oceanogr.*, **40**, 1942–1964.
- Wahl, S., M. Latif, W. Park, and N. Keenlyside, 2011: On the tropical Atlantic SST warm bias in the Kiel Climate Model. *Climate Dyn.*, **36**, 891–906, doi:10.1007/s00382-009-0690-9.
- Xie, P., and P. A. Arkin, 1997: Global precipitation: A 17-year monthly analysis based on gauge observations, satellite estimates, and numerical model outputs. *Bull. Amer. Meteor. Soc.*, **78**, 2539–2558.
- Xie, S.-P., and J. A. Carton, 2004: Tropical Atlantic variability: Patterns, mechanisms, and impacts. *Earth's Climate: The Ocean-Atmosphere Interaction*, *Geophys. Monogr.*, Vol. 147, Amer. Geophys. Union, 121–142.
- Zeng, N., R. E. Dickinson, and X. Zeng, 1996: Climatic impact of Amazon deforestation—A mechanistic model study. *J. Climate*, **9**, 859–883.
- Zheng, Y., T. Shinoda, J.-L. Lin, and G. N. Kiladis, 2011: Sea surface temperature biases under the stratus cloud deck in the southeast Pacific Ocean in 19 IPCC AR4 coupled general circulation models. *J. Climate*, **24**, 4139–4164.
- Zuidema, P., D. Painemal, S. de Szoëke, and C. Fairall, 2009: Stratocumulus cloud-top height estimates and their climatic implications. *J. Climate*, **22**, 4652–4666.